JOURNAL OF Applied Polymer SCIENCE

Synthesis, Characterization, and Swelling Kinetics of pH-Responsive and Temperature-Responsive Carboxymethyl Chitosan/Polyacrylamide Hydrogels

Qing-Bo Wei,[1] Yan-Ling Luo,[2] Feng Fu,[1] Yu-Qi Zhang,[1] Rong-Xuan Ma[1]

[1]Key Laboratory of Chemical Reaction Engineering of Shaanxi Province, College of Chemistry and Chemical Engineering, Yan'an University, Yan'an 716000, People's Republic of China

[2]Key Laboratory of Macromolecular Science of Shaanxi Province, School of Chemistry and Chemical Engineering, Shaanxi Normal University, Xi'an 710062, People's Republic of China

Correspondence to: Y.-L. Luo (E-mail: luoyanl@snnu.edu.cn)

ABSTRACT: A novel pH- and temperature-responsive hydrogel composed of carboxymethyl chitosan (CMC) and polyacrylamide (PAM) semi-interpenetrating polymer networks (semi-IPNs) was synthesized by a crosslinking copolymerization route in the presence of *N*,*N*-methylene bisacrylamide and potassium persulfate. The structure of the CMC/PAM hydrogels was characterized by Fourier transform infrared spectroscopy, and the morphologies were observed by scanning electron microscopy. The swelling kinetics investigations demonstrated that the equilibrium swelling ratios (ESRs) of the semi-IPN hydrogels depended on the compositional ratios, pH values of the buffer solutions, and temperature. The ESR values increased with increasing CMC contents and pH values; this was in agreement with the maximum theoretical water contents fitted by the swelling kinetic data. The CMC/PAM hydrogels complied with Fickian behavior at pH 1.4 and non-Fickian behavior at pH 11.7 in the buffer solutions. These hydrogels displayed thermosensitivities that were different from those of common thermoresponsive gels. The swelling was enhanced when the temperature of the media was increased up to 40°C; this was followed by a reduction. Therefore, the swelling behavior of the CMC/PAM hydrogels could be controlled and modulated by means of the compositional ratios of CMC to acrylamide, pH values of the buffer solutions, and temperature. © 2012 Wiley Periodicals, Inc. J. Appl. Polym. Sci. 129: 806–814, 2013

KEYWORDS: biomaterials; gels; kinetics; stimuli-sensitive polymers; swelling

Received 22 September 2012; accepted 30 October 2012; published online 15 December 2012

DOI: 10.1002/app.38788

INTRODUCTION

Hydrogels are polymeric networks that can absorb large quantities of water while remaining insoluble in aqueous solutions because of the chemical or physical crosslinking of individual polymer chains.[1,2] They undergo a volume phase change in response to a change in the external stimuli, such as the pH, ionic strength, temperature, electric filed, solvent, pressure, or light intensity.[3–9] They have been demonstrated to induce abrupt changes in the physical and chemical properties. All of these properties of hydrogels make them important materials in controlled drug delivery, tissue culture substrates, molecular separation, and several technical applications.[10–15] Chitosan is a copolymer of D-glucosamine and *N*-acetyl glucosamine and is derived from chitin. It has been reported that chitosan is a potentially useful pharmaceutical material because of its good biocompatibility and low toxicity.[16–18] For drug-delivery applications, chitosan needs to be crosslinked because of its hydrophilic properties. On the other hand, it is well known that polyacrylamide (PAM) is typically a kind of linear-type water-soluble polymer whose hydrogels respond to possess pH responsiveness after hydrolyzation,[19,20] temperature sensitivities in the presence of *N*,*N*′-methylene bisacrylamide (NNMBA),[21] and good biocompatibility. More recently, many studies have been conducted to fabricate and characterize hydrogels with dual sensitivities. This is accomplished by the copolymerization of a temperature-sensitive monomer, usually *N*-isopropyl acrylamide, and a pH-sensitive monomer, such as acrylic acid or methacrylic acid.[22–27]

Considering the aforementioned description, we synthesized novel pH-responsive and thermoresponsive PAM/carboxymethyl chitosan (CMC) semi-interpenetrating network (semi-IPN) hydrogels and characterized them by Fourier transform infrared (FTIR) spectroscopy and scanning electron microscopy (SEM). The swelling response of the hydrogels was studied as a function

© 2012 Wiley Periodicals, Inc.

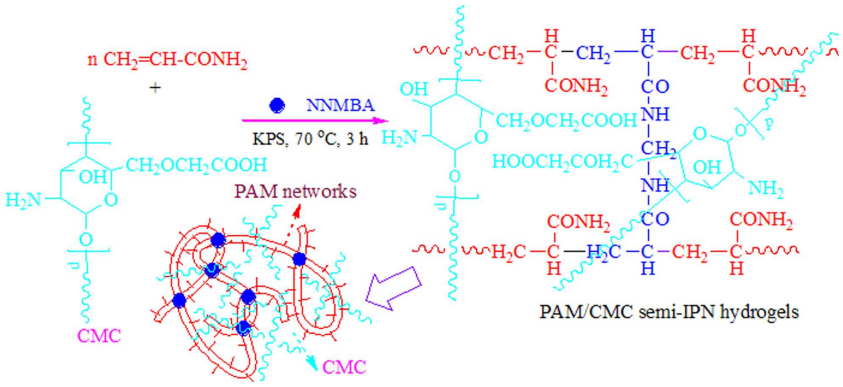

Scheme 1. Schematic demonstrating the synthesis of the CMC/PAM semi-IPN hydrogels. [Color figure can be viewed in the online issue, which is available at wileyonlinelibrary.com.]

of the time, temperature, pH, and ionic strength. The swelling dynamics of the hydrogels are discussed to evaluate the diffusion mechanism. They are expected to find wide applications in specific biomedical fields, such as drug controlled release.

EXPERIMENTAL

Materials and Reagents

Chitosan (CS), with degree of deacetylation of 80% and a molecular weight of 1.0×10^6, was obtained from the Shandong Chemical Factory (Weifang, China). Acrylamide (AM; analytical grade) was supplied by the Shantou Xianhua Chemicals Factory (Shantou, China). The crosslinker, NNMBA (analytical grade), was purchased from the Tianjin Kermol Chemical Regent Developing Center (Tianjin, China). Potassium persulfate (KPS) as an initiator, supplied by the Xi'an Chemical Reagent Factory (Xi'an, China), was recrystallized before use. Phosphate buffers with various pH values of 1.4, 2.8, 7.4, 8.8, and 11.7 as physiological media were prepared with Na_2HPO_4, NaH_2PO_4, HCl, and H_3PO_4 to examine the swelling behavior, and NaCl was used to adjust the ionic intensities.

Preparation of CMC

Purified chitosan (10.0 g) was added to 50 mL of a 50 wt % NaOH solution at 20°C overnight for alkalization. After the excessive alkali solution was extruded, the chitosan was put into a 250-mL reactor. Afterward, chloroacetic acid (10.0 g) dissolved in 40.0 mL of isopropyl alcohol was added dropwise to the system. After the mixture solution was refluxed at 60°C under intense stirring for 4 h, the solvent was discarded. Next, the mixture was neutralized with alcohol and precipitated in acetone.[28] The product was carefully washed by acetone three times and then dried in an oven at 35°C until a constant weight was reached, and the CMC was obtained.

Preparation of the CMC/PAM Semi-IPN Hydrogels

CMC/PAM semi-IPN hydrogels were synthesized with a free-radical crosslinking copolymerization approach in the presence of both CMC and AM, and the synthesizing strategy is displayed in Scheme 1. The formula compositions and codes used in our study are shown in Table I.

Typically, in line with Table I, a stoichiometric amount of CMC was dissolved in 10 mL of deionized water to form a viscous solution, and then, a stoichiometric amount of AM monomer was added to the aforementioned CMC solution. After it was stirred at 60°C for about 10 min, 0.02 g of potassium persulfate and 0.02 g of NNMBA (1 wt % of the total weight of the monomer) were added to the reaction mixture with rapid stirring. The reaction proceeded at 60°C for about 2 h. The products were immersed in deionized water for 7 days to remove residues of the unreacted monomers and crosslinking agents. The resulting hydrogels were dried in an oven at 35°C until a constant weight was reached.

Characterization and Measurements

The structural characterization of the CMC/PAM hydrogels was carried out with the method of potassium bromide tableting on an EQUINX55 FTIR spectroscope manufactured by the Bruker Corp (Karlsruhe, Germany). The morphological observation of the samples was conducted on a Quanta 200 scanning electron microscope (Philips-FEI Corp, Eindhoven, The Netherlands), with an operating voltage of 20 kV. To understand swelling of the CMC/PAM hydrogels, the dried hydrogels [dried hydrogel weight (W_0)] were immersed in excess deionized water at room temperature (25°C) until a swelling equilibrium was attained. The wet weight of the sample (W_t) was determined after the removal of the surface water by blotting with filter paper, and the equilibrium water content (EWC) was designated as W_∞. The swelling ratio (S_R) and equilibrium swelling ratio (ESR) of the samples were calculated from the following equations:

$$S_R = (W_t - W_0)/W_0 \quad (1)$$

$$\mathrm{ESR} = (W_\infty - W_0)/W_0 \quad (2)$$

Table I. Proportions of the Various Ingredients Used in the Synthesis of the Hydrogels

Sample[a]	A	B	C	D	E
Ratio of CMC to AM (w/w %)	5 : 95	10 : 90	20 : 80	30 : 70	35 : 65

Applied Polymer SCIENCE

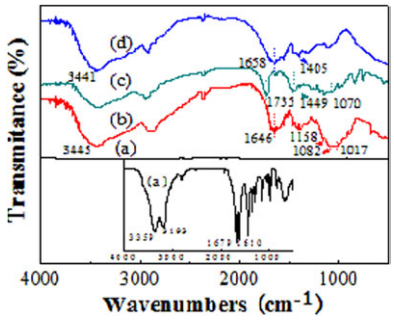

Figure 1. FTIR spectra of the (a) PAM, (b) CS, (c) CMC, and (d) CMC/PAM hydrogel. [Color figure can be viewed in the online issue, which is available at wileyonlinelibrary.com.]

RESULTS AND DISCUSSION

FTIR Analysis

Figure 1 illustrates the FTIR spectra of PAM, chitosan, CMC, and the CMC/PAM hydrogels. Because the transmittance was low, the FTIR spectrum of PAM as an insert was simultaneously incorporated into Figure 1. As shown in inset (a) of Figure 1, the relatively strong vibration band at about 3359 cm^{-1} corresponded to the symmetrical stretching vibration absorption peak of —NH_2 groups on the PAM chains, and the shoulder peak at 3193 cm^{-1} was attributable to —NH_2 stretching in the PAM molecules in the hydrogen-bonding state. The characteristic peaks at 1679 and 1610 cm^{-1} were assigned to the carbonyl group (—C=O) stretching vibration and the N—H bending vibration of amide groups, respectively.[29,30] In the IR spectrum shown in Figure 1(b), chitosan showed three peaks at 1017, 1082, and 1158 cm^{-1}, which were characteristic peaks of the saccharide structure. A broad peak around 3445 cm^{-1} was assigned to the O—H and N—H stretching vibrations of the polysaccharide. The appearance of amide absorption peaks at 1646 and 1380 cm^{-1} indicated that chitosan had a very high deacetylation degree.[28,31] In the IR spectrum of CMC, the peak at 1449 cm^{-1} was assigned to the symmetrical stretching vibration of —COO, and the strong absorption peak at 1735 cm^{-1} was attributable to the overlapping of the asymmetrical stretching vibration of —COO and the deforming vibration of —NH_2. The C—O absorption peak of a secondary hydroxyl group moved to 1070 cm^{-1}. The results indicate that the carboxymethylization reaction occurred. In the IR spectrum shown in Figure 1(d), the existence of peaks at 3441 and 1658 cm^{-1} was due to the cocontribution of CMC and PAM in the CMC/PAM hydrogel and was attributable to the superposition of asymmetric —NH_2 stretching and —OH stretching vibrations as well as carbonyl stretching, respectively. The symmetrical stretching vibrations of the —COO^- groups were located at 1405 cm^{-1}. All of this corroborated the formation of the CMC/PAM hydrogels.

SEM Observations

The porous structure of these materials will be beneficial to the diversion of the fluid when they are employed as biomaterials. To investigate the morphologies of the hydrogels, the as-prepared hydrogels were fractured after lyophilization and plated with a thin layer of gold on their cross sections, and SEM was used to observe the fractured morphologies of the freeze-dried hydrogels, as shown in Figure 2. The SEM micrographs clearly illustrate that the morphologies of the hydrogels may have been correlated with their compositions to some extent. As shown in Figure 2, the three-dimensional pores in the SEM picture changed significantly, depending on their chemical compositions. In the presence of the same NNMBA concentration, with increasing CMC content in the hydrogel composition, the porous structure became laxer, and the pore size got bigger. When the CMC content was over 30 wt %, the porous walls of the hydrogels shown in Figure 2(d,e) became thicker than those in shown in Figure 2(a–c). These results signify that the component and the feed ratios were directly related to the topologies of the hydrogels. This morphological feature had an important impact on swelling of the synthesized CMC/PAM hydrogels.

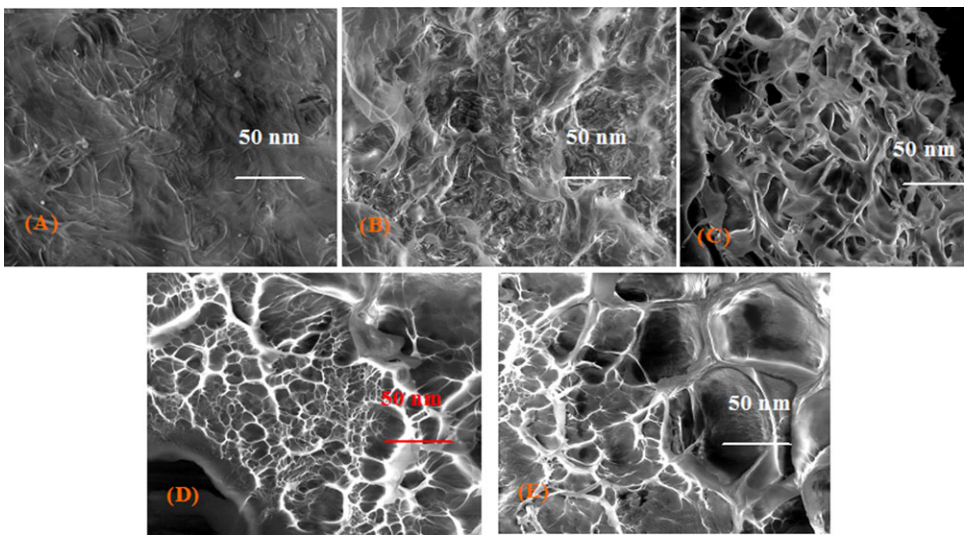

Figure 2. SEM photographs of various hydrogels with different CMC contents. The mass ratios of CMC to AM were (A) 5 : 95, (B) 10 : 90, (C) 20 : 80, (D) 30 : 70, and (E) 35 : 65. [Color figure can be viewed in the online issue, which is available at wileyonlinelibrary.com.]

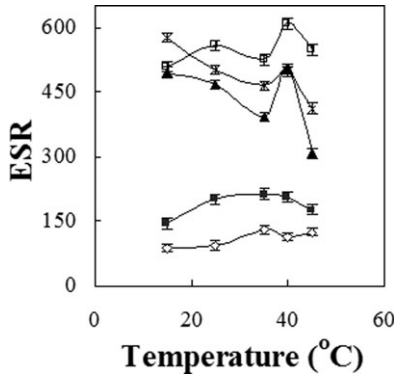

Figure 3. Effect of the mass content of CMC and the temperature on the EWC of the CMC/PAM hydrogels with CMC contents of (◇) 5, (■) 10, (▲) 20, (□) 30, and (*) 35 wt %.

Thermoresponsive Properties

It is well known that hydrogels with a suitable hydrophilic–hydrophobic balance may exhibit thermosensitivity.[32] Hydrogel systems having the association/dissociation characteristics of the hydrogen bonding between polar groups within semi-IPNs or IPNs also show a temperature-responsive swelling behavior.[33] In most cases, PAM itself is generally believed not to exhibit temperature sensitivities. However, Neamtu et al.[34] reported a temperature dependence of the swelling degree for PAM hydrogels prepared with different NNMBA contents. This behavior was also found in our experiments, as shown in Figure 3. They only showed a moderate temperature response, which may have been due to the absence of hydrophobic groups in the side chains of PAM. The ESR values of the CMC/PAM hydrogels in deionized water varied slightly with temperature but changed remarkably with the CMC content. The ESR values were enhanced from 60 to 800 with increasing CMC content in the hydrogel compositions, corresponding to the three-dimensional porous topologies observed in Figure 2. In particular, for the hydrogels with 10 and 20 wt % CMC, the change was even more obvious. Below 10 wt % CMC, the ESR values increased slightly up to about 35°C; this was followed by a slight decrease in swelling. In contrast, when the CMC content was increased above 20 wt %, the swelling first decreased and then swiftly increased with increasing temperature of the media from 35 to 40°C; this was followed by a remarkable reduction. In other words, the hydrogels that included a large amount of CMC showed some temperature response, whereas the gels with low CMC contents did not show any evident response. Therefore, we speculated that the temperature response of the hydrogels may have come predominately from CMC, not just the PAM network.

The decrease in swelling that resulted from an increase in temperature may be explained by the thermodynamic aspects. It is well known that the entropy of mixing between polymers and water decreases because of the formation of cage structures and the enhancement of the order degree of water molecules. Therefore, ΔS was negative, and ΔH was also negative because of the formation of hydrogen bonds and the previous exothermic swelling process.[35–37] According to $\Delta G = \Delta H - T\Delta S$, ΔG is defined as Gibbs free energy; ΔH is defined as enthalpy and ΔS is defined as entropy, an increase in the temperature leads to larger negative $T\Delta S$ values, and the ΔG values are then increased; this is disadvantageous for the swelling of the hydrogels. To more deeply understand the effect of the temperature on the swelling properties, the logarithm of EWC {EWC = $[(W_\infty - W_0)/W_\infty)]\%$} was plotted against the reciprocal of the swelling medium temperature, as depicted in Figure 4. For five hydrogels with different CMC contents, the EWC values are tabulated in Table II; these values decreased with temperature. According to the Gibbs–Helmholtz equation for EWC, the relationship between ln EWC and $1/T$ follows the Gibbs–Helmholtz equation:[38,39]

$$d\ln \mathrm{EWC}/d(1/T) = -\Delta H_m/R \tag{3}$$

where T is defined as temperature in Kelvin; R is the gas constant (8.314 J K^{-1} mol^{-1}) and ΔH_m is the enthalpy of mixing between the dry polymer and an infinite amount of water. It could be seen that the data points fit well to the straight line in Figure 4. ΔH_m of every sample was obtained according to the slope of each line, as listed in Table III. The negative values of ΔH_m indicated that the swelling process of the CMC/PAM copolymers was exothermic, and the value of ΔH_m was dependent on the copolymer composition and increased with increasing CMC content.

Ionic Strength and pH Response

The capacity of swelling is one of the most important parameters in the evaluation of the properties of hydrogels. For ionic hydrogels, the degree of swelling not only depends on the chemical compositions of the polymers but also responds to changes in the external pH. The equilibrium swelling of ionic hydrogels is determined by a balance of three primary forces: (1) the free energy of mixing of the network chains with the swelling medium, (2) the elastic retractile force of the network chains, and (3) the ionic osmotic pressure resulting from mobile counterions surrounding the fixed charged groups of the networks.[40] In other words, an appropriate balance of hydrophilicity and hydrophobicity in the molecular structure of the polymer chain is believed to be the key component in the phase-transition behavior of the corresponding polymer networks.[41–45]

In this study, we investigated the ionic strength effect with a collection of buffer solutions with various ionic strengths of 0.2,

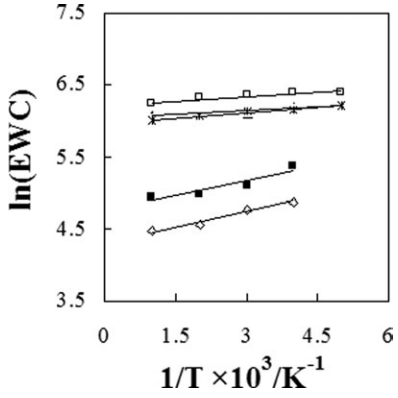

Figure 4. Temperature dependence of EWC for various hydrogels with CMC contents of (◇) 5, (■) 10, (▲) 20, (□) 30, and (*) 35 wt %.

Table II. Dependence of the EWC Values of the Hydrogels on the Temperature and CMC Contents

	CMC content (wt %)				
	5	10	20	30	35
T (K)	EWC (wt %)				
288	98.877	99.285	99.7716	99.8044	99.7524
298	98.962	99.311	99.7744	99.8214	99.7689
303	99.162	99.389	99.7784	99.8275	99.7826
308	99.243	99.53	99.7943	99.8327	99.7855

0.4, 0.6, 0.8, and 1.0 (pH 7.4), as depicted in Figure 5. The xerogels were swollen in aqueous solutions with various NaCl concentrations, and the S_R values were determined. Figure 5 shows the variation of S_R values with different ionic strengths and CMC contents for the hydrogels. With a pK_a value of 2.3 for the —COOH groups and a pK_b value of 6.5–6.6 for the —NH_2 groups in the CMC structure,[46,47] NH^{3+} and COOH could exist in strongly acidic media, NH_2 and COO^- could exist at pH values above 7, and NH^{3+} and COO^- or NH_2 and COOH were present at pH values of 3.5–7. Consequently, it was clear that the ionic strength effect on swelling was related not only to the CMC content but also to the existing NH_2 and COO^- groups at pH 7.4. Above a 20 wt % CMC content, as the ionic strength (NaCl concentration) of the swelling media increased, the S_R values of the hydrogels decreased accordingly. This well-known phenomenon, commonly observed in the swelling of ionic hydrogels, is often attributed to a charge screening effect of the additional cations, which causes a nonperfect anion–anion electrostatic repulsion and leads to a decreased osmotic pressure difference between the hydrogel network and the external solution. The swelling loss was attributed to the charge screening effect of the cations and led to the reduction of osmotic pressure and the driving force for swelling between the gel and the aqueous phases. Therefore, although the COO^-–COO^- electrostatic repulsion stemming from the COOH groups of CMC promoted swelling, the screening effect from counterions greatly impaired the repulsion. Below 10 wt % CMC, the S_R values did not exhibit any noticeable change with ionic strength; this may have been due to a complete screening effect at low —COOH contents, which counteracted the contribution of the COO^-–COO^- electrostatic repulsion.

A pH-dependent swelling behavior was observed in different pH buffer solutions at room temperature, as shown in Figure 6. The CMC/PAM semi-IPNs were ionized hydrogels, in that their swelling behavior depended on the characteristics of both the chemical structure and the medium. In this experiment, the hydrogel samples contained —$CONH_2$, —NH_2 (basic), and —COOH (acidic) groups. Therefore, the swelling change in the CMC/PAM semi-IPNs hydrogels with pH was expected to be influenced by charge density changes in the polymers caused by the —NH_2 and —COOH group disintegration degrees at different pH values and the CMC contents. Under highly acidic conditions at pH values below 3.5, the acidic and basic groups appeared as NH^{3+} and COOH, and thus, the hydrogels contracted and deswelled because of the intramolecular and/or intermolecular hydrogen bond interactions between PAM and CMC. Although there were NH^{3+} cations in this case, the countraion Cl^- may have shielded the charge of the NH^{3+} cations and prevented an efficient NH^{3+}–NH^{3+} repulsion and led to decreased swelling. As pH increased, the partially protonated (NH^{3+}) and/or deprotonated (COO^-) groups gradually increased the charge density on the polymer chains and caused an enhancement of the osmotic pressure inside the gel particles due to the gradually increased double NH^{3+}–NH^{3+} or COO^-–COO^- electrostatic repulsion. Then, the hydrogels swelled. Notably, there could be simultaneous hydrogen bonding between NH_2, —$CONH_2$, and —COOH or NH^{3+}–COO^- as these groups were ionized from pH 3.5 to 7.4, which resulted in decreased swelling. The increased swelling was a result of the combined effects of hydrogen bonding, electrostatic repulsion, and the screening effect. The S_R values arrived at a maximum at a pH of 7.4 because of strong electrostatic repulsion interactions from the highly ionized pendant carboxyl groups (COO^-) in the CMC chains. The slight decrease in swelling above pH 7.4 may have been due to the high charge screening effect of excess counter ions of Na^+. The effect of various disintegration degrees

Table III. ΔH_m Values for Various Hydrogels

Sample	A	B	C	D	E
CMC content (w/w %)	5	10	20	30	35
ΔH_m (J/mol)	−1.1723	−1.1748	−0.3143	−0.3475	−0.414

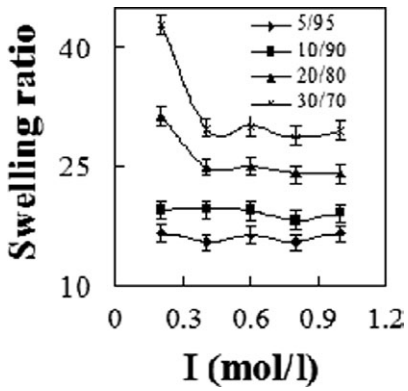

Figure 5. Effect of the ionic strength (I) on ESR at pH 7.4 and at room temperature with CMC contents of (◇) 5, (■) 10, (▲) 20, and (□) 30 wt %, respectively.

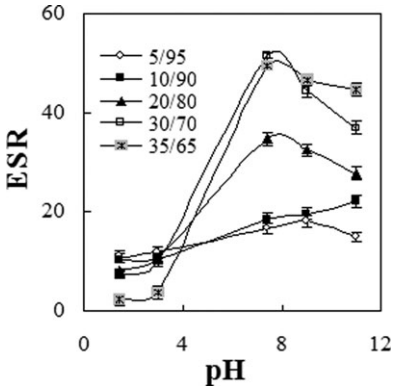

Figure 6. S_R values of the CMC/PAM samples in different buffer solutions and at room temperature with CMC contents of (◇) 5, (■) 10, (▲) 20, (□) 30, and (*) 35 wt %.

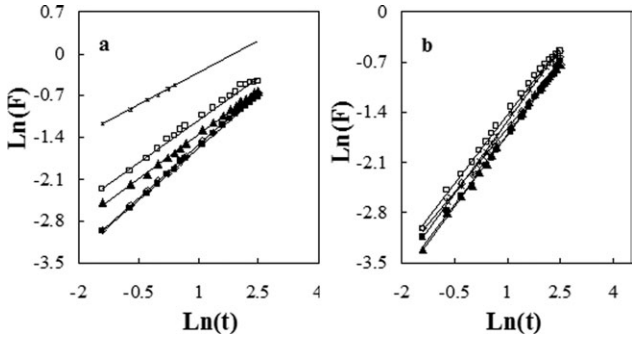

Figure 8. Ln F versus ln t of the CMC/PAM hydrogels under various mass ratios in buffer solutions at pH values of (a) 1.4 and (b) 11.7 and at 25°C with CMC contents of (◇) 5, (■) 10, (▲) 20, (□) 30, and (*) 35 wt %.

of ionic groups in CMC, such as —NH_2 and —COOH groups, on swelling were further demonstrated by the various CMC contents. When the CMC/AM composition was up to 35 wt %, more —COOH and —NH_2 groups on the CMC side chains resulted in the highest swelling. However, when the mass ratio of CMC to AM was below 10%, changes in the swelling with pH were not obvious.

To sum up, the CMC/PAM semi-IPN hydrogels showed both pH and ionic strength sensitivities, and the ionic groups of CMC, such as COO^- and NH^+_3 groups, played the main role in swelling variations; this led to different ESRs in the gels at different pH and ionic strength values.

Swelling Kinetics Analysis

Generally, the swelling of hydrogels involves a water diffusion process into the hydrogel and a larger scale segmental motion, which ultimately results in an increase of the separation distance among hydrogel chains. Diffusion involves the migration of water into preexisting or dynamically formed spaces among hydrogel chains. Figure 7 shows the time-dependent swelling behaviors of the CMC/PAM hydrogels with various CMC contents in different buffer solutions at room temperature. It was clear that the swelling of the hydrogels gradually increased with time, and in PBS at pH 7.4, the fastest swelling rate was observed and was due to the COO^-–COO^- electrostatic repulsion of CMC. The swelling rates increased with increasing CMC contents in PBS at pH values of 7.4 and 11.7. On the contrary, for the hydrogels at pH 1.4, the swelling rate decreased because of hydrogen-bonding interactions between the protonation of carboxyl groups and charge screening.

To elucidate the diffusion model of the gel so as to understand nature of swelling, the initial swelling data at pHs of 1.4 and 11.7, as shown in Figure 7, were fitted to the exponential heuristic equation for $S/S_\infty \leq 0.6$:[48–50]

$$F = S/S_\infty = kt^n \text{or} \ln\ F = \ln\ k + n \ln t \quad (4)$$

where F is the water fraction at time t; S and S_∞ are the amounts of water absorbed by the hydrogel at time t and in the equilibrium state, respectively; k is a characteristic constant of the hydrogel; and n is a characteristic exponent of the mode of transportation or penetration. The constant n and k were calculated from the slopes and intercepts of the graph of ln F against ln t for the hydrogels in different buffer solutions. For the first case, $n \leq 0.5$, corresponding to Fickian diffusion, the rate of diffusion was much lower than the rate of relaxation, and for the second, $n = 1$, the diffusion was very fast, in contrast to the rate of relaxation. The third case corresponded to an anomalous diffusion with n values between 0.5 and 1. These results are shown in Figure 8 and Table IV. The numerical value n provides information about the mechanism of swelling kinetics. It can be seen that the transport mechanism belonged to Fickian diffusion or the anomalous diffusion mode in pH 1.4 buffer solution for the CMC/PAM hydrogels at 25°C; this depended on the

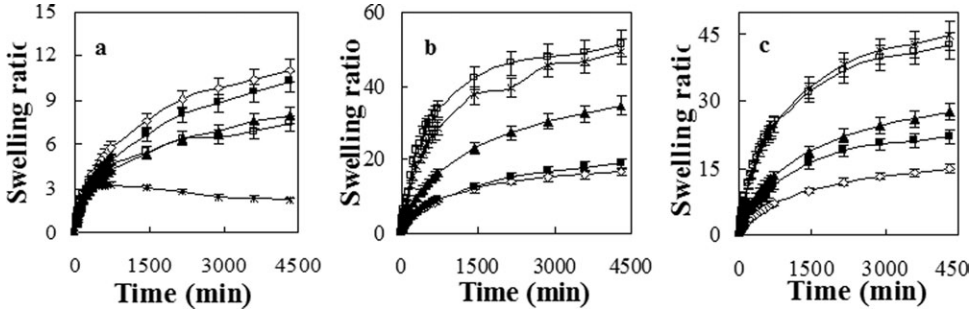

Figure 7. S_R values of various CMC/PAM hydrogel samples in different buffer solutions and at room temperature at pH values of (a) 1.4, (b) 7.4, and (c) 11.7 with CMC contents of (◇) 5, (■) 10, (▲) 20, (□) 30, and (*) 35 wt %.

Table IV. Swelling Kinetic Equations and Kinetic Parameters of the CMC/PAM Hydrogel Samples in Buffer Solution at 25°C

Buffer solution	Initial swelling	R^2	n	ln k
pH 1.4	ln F_A = 0.6025 Ln t − 2.1269	0.9995	0.6025	−2.1269
	ln F_B = 0.5887 Ln t − 2.1675	0.9994	0.5887	−2.1675
	ln F_C = 0.5887 Ln t − 1.8425	0.9989	0.4949	−1.8425
	ln F_D = 0.4769 5887 Ln t − 1.5876	0.9959	0.4769	−1.5876
	ln F_E = 0.35855887 Ln t − 0.684	0.9996	0.3585	−0.684
pH 11.7	ln F_A = 0.5945 5887 Ln t − 2.2268	0.9989	0.5945	−2.2268
	ln F_B = 0.6452 5887 Ln t − 2.3664	0.9966	0.6452	−2.3664
	ln F_C = 0.67455887 Ln t − 2.3747	0.9992	0.6745	−2.3747
	ln F_D = 0.64075887 Ln t − 2.0742	0.9974	0.6407	−2.0742
	ln F_E = 0.6766 5887 Ln t − 2.2012	0.9975	0.6766	−2.2012

The subscripts *A*, *B*, *C*, *D*, and *E* represent mass ratios of CMC to AM of 5 : 95, 10 : 90, 20 : 80, 30 : 70, and 35 : 65, respectively.

mass ratios of CMC to AM. The dynamic swelling behavior of the CMC/PAM hydrogels in pH 11 buffer solutions, however, complied with the non-Fickian diffusion mode. In this case, the polymer chain relaxation played a major role in swelling. The initial swelling process exhibited Fickian or non-Fickian behavior, and the extensive swelling process followed the Schott second-order dynamic equation:[51]

$$dS/dt = k_s(S_\infty - S)^2 \quad (5)$$

$$t/S = A + Bt \quad (6)$$

where A and B are constants related to the maximal theoretical water contents and can be expressed as $A = 1/k_s S_\infty{}^2 = 1/[dS/dt)_0]$ and $B = 1/S_\infty$, respectively, and k_s is the swelling rate constant. The reciprocal of the constant A is defined as the initial swelling rate ($r_0 = 1/A$). The constants B and A were calculated from the slopes and intercepts of the plots of t/S versus t curves for hydrogels with various compositional proportions, as shown in Figure 9. The swelling kinetic equations and the r_0 and S_∞ values of the CMC/PAM hydrogel samples are tabulated in Table V. All of the R^2 values were greater than 0.999; this indicated a small estimated standard error and a high precise linear regression equation. With increasing CMC proportion in the hydrogels, S_∞ was reduced in the pH 1.4 buffer solutions,

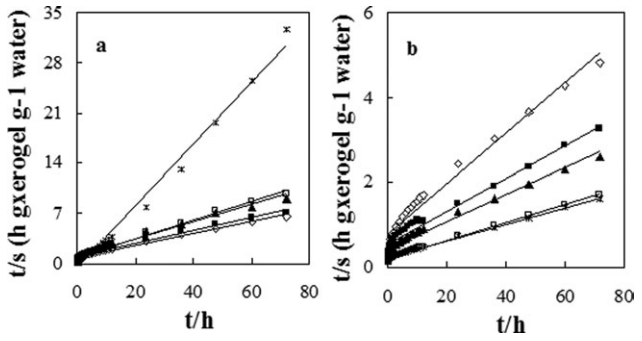

Figure 9. t/S versus t curves of the CMC/PAM hydrogels under various mass ratios in buffer solutions at pH values of (a) 1.4 and (b) 11.7 and at 25°C with CMC contents of (◇) 5, (■) 10, (▲) 20, (□) 30, and (*) 35 wt %.

Table V. Extensive Swelling Kinetic Equations, r_0 Values, and Maximum Theoretical Water Contents (S_∞'s) of the CMC/PAM Hydrogel Samples in PBS Solution at 25°C

Buffer solution	Extensive swelling	S_∞ (g of water/g of xerogel)	r_0 [g of water (g of xerogel)$^{-1}$ min^{-1}]	k_s [g of water (g of gel)$^{-1}$ min^{-1}]
pH = 1.4	$(t/S)_A$ = 0.0827t + 0.887	12.09	1.13	164.84
	$(t/S)_B$ = 0.0897t + 1.0381	11.15	0.96	119.72
	$(t/S)_C$ = 0.1197t + 1.0182	8.35	0.98	68.55
	$(t/S)_D$ = 0.1326t + 0.7337	7.54	1.36	77.52
	$(t/S)_E$ = 0.4302t − 0.4947	2.32	2.02	10.92
pH = 11.7	$(t/S)_A$ = 0.0597t + 0.7637	16.75	1.31	367.39
	$(t/S)_B$ = 0.0381t + 0.5644	26.25	1.77	1220.57
	$(t/S)_C$ = 0.0315t + 0.4358	31.75	2.29	2312.55
	$(t/S)_D$ = 0.0213t + 0.1957	46.95	5.11	11,262.89
	$(t/S)_E$ = 0.02t + 0.2099	50.00	4.76	11,910.43

The subscripts *A*, *B*, *C*, *D*, and *E* represent mass ratios of CMC to AM of 5 : 95, 10 : 90, 20 : 80, 30 : 70, and 35 : 65, respectively.

whereas the value increased in the pH 11 buffer solution. The theoretically fitted results were in good agreement with the experimental data. Therefore, the compositional ratios and the medium could be employed to modulate the swelling behavior.

CONCLUSIONS

In summary, we have demonstrated a simple method for the synthesis of novel pH- and temperature-responsive CMC/PAM semi-IPN hydrogels. The intermolecular hydrogen-bonding interactions were confirmed by FTIR spectroscopy and were proven to have an impact on the topologies of the as-synthesized hydrogels. The morphologies and swelling response of the CMC/PAM hydrogels were modulated and controlled by the variation of the molar compositions of CMC and AM. The swelling behavior of the hydrogels was closely related to charge density changes in the polymers caused by the groups of —NH_2 and —COOH disintegrating at different pH values as well as the CMC contents, and the swelling kinetics depended not only on the pH but also on the compositions of the external solutions. An increase in the ionic strength of the swelling medium or the temperature resulted in a decrease in W_∞. The hydrogels exhibited thermoresponsive properties in aqueous solutions at 35–40°C to some extent, depending on the system composition. The values of ΔH_m between the polymer and water were obtained for five hydrogels with different compositions; these values were negative and increased with increasing CMC content. The proximity to physiological temperature opens some possibilities for the application of these copolymers in drug delivery. Under two buffer solution conditions, the transport mechanism belongs to Fickian or non-Fickian transport for the CMC/PAM hydrogels, and the extensive swelling process follows the Schott second-order dynamic equation, of which the polymer chain relaxation plays a major role in the rate of swelling.

ACKNOWLEDGMENT

The authors appreciate the financial support from the Natural Science Foundation of China (contract grant number 21103146).

REFERENCES

1. Kim, S. J.; Park, S. J.; Kim, S. I. *React. Funct. Polym.* **2003**, *55*, 61.
2. Vashist, A.; Gupta, Y. K.; Ahmad, S. *Carbohydr. Polym.* **2012**, *87*, 1433.
3. Chang, C. Y.; He, M.; Zhou, J. P.; Zhang, L. N. *Macromolecules* **2011**, *44*, 1642.
4. Tang, Y. F.; Du, Y. M.; Hu, X. W.; Shi, X. W.; Kennedy, J. F. *Carbohydr. Polym.* **2007**, *67*, 491.
5. Chiu, H. C.; Lin, Y. F.; Hung, S. H. *Macromolecules* **2002**, *35*, 5235.
6. Yamamoto, K.; Serizawa, T.; Akashi, M. *Macromol. Chem. Phys.* **2003**, *204*, 1027.
7. Aouada, F. A.; de Moura, M. R.; Orts, W. J.; Mattoso, L. H. C. *J. Agric. Food Chem.* **2011**, *59*, 9433.
8. Zhao, Y.; Su, H.; Fang, L.; Tan, T. *Polymer* **2005**, *46*, 5368.
9. Kato, E. *J. Appl. Polym. Sci.* **2005**, *95*, 1069.
10. Jin, S. P.; Liu, M. Z.; Zhang, F.; Chen, S. L.; Niu, A. Z. *Polymer* **2006**, *47*, 1526.
11. Ribeiro, A.; Veiga, F.; Santos, D.; Torres-Labandeira, J. J.; Concheiro, A.; Alvarez-Lorenzo, C. *Biomacromolecules* **2011**, *12*, 701.
12. Caykara, T.; Kiper, S.; Demirel, G. *Eur. Polym. J.* **2006**, *42*, 348.
13. Minett, A.; Fràysse, J.; Gang, G.; Kim, G. T.; Roth, S. *Curr. Appl. Phys.* **2002**, *2*, 61.
14. Vohrer, U.; Kolaric, I.; Haque, M. H.; Roth, S.; Weglikowska, U. D. *Carbon* **2004**, *42*, 1159.
15. Hoare, T. R.; Kohane, D. S. *Polymer* **2008**, *49*, 1993.
16. Mi, F. L.; Tan, Y. C.; Liang, H. F.; Sung, H. W. *Biomaterials* **2002**, *23*, 181.
17. Lee, J.; Choi, C. S.; Hwa Shin, S.; Seok Ban, H.; Rhim, T.; Lee, S. K.; Lee, K. Y. *Bioconjugate Chem.* **2012**, *23*, 1174.
18. Chen, S. C.; Wu, Y. C.; Mi, F. L.; Lin, Y. H. *J. Controlled Release* **2004**, *96*, 285.
19. Zhao, Q.; Sun, J.; Lin, Y.; Zhou, Q. *React. Funct. Polym.* **2010**, *70*, 602.
20. Turan, E.; Demirci, S.; Caykara, T. *J. Appl. Polym. Sci.* **2009**, *111*, 108.
21. Neamtu, I.; Chiriac, A. P.; Nita, E. *J. Optoelectron. Adv. Mater.* **2006**, *8*, 1939.
22. Patenaude, M.; Hoare, T. *Macromol. Lett.* **2012**, *1*, 409.
23. Prior-Cabanillasa, A.; Quijada-Garrido, I.; Frutosb, G.; Barrales-Riendaa, J. M. *Polymer* **2005**, *46*, 685.
24. Gümüşderelioğlu, M.; Topal, I. *U. Radiat. Phys. Chem.* **2005**, *73*, 272.
25. Yuan, C. H.; Lin, S. B.; Liu, B.; Ke, A. R.; Quan, Z. L. *Sens. Actuators B* **2009**, *140*, 155.
26. Panic, V.; Adnadjevic, B.; Velickovic, S.; Jovanovic, J. *Chem. Eng. J.* **2010**, *156*, 206.
27. Liang, H. F.; Hong, M. H.; Ho, R. M.; Chung, C. K.; Lin, Y. H.; Chen, C. H.; Sung, H. W. *Biomacromolecules* **2004**, *5*, 1917.
28. Sun, T.; Xu, P. X.; Liu, Q.; Xue, J.; Xie, W. M. *Eur. Polym. J.* **2003**, *39*, 189.
29. Şanlı, O.; Ay, N.; Işıklan, N. *Eur. J. Pharm. Biopharm.* **2007**, *65*, 204.
30. Liu., Z. Q.; Luo, Y. L.; Zhang, K. P. *J. Biomater. Sci. Polym. Ed.* **2008**, *19*, 1503.
31. Chen, S. C.; Wu, Y. C.; Mi, F. L.; Lin, Y. H.; Yu, L. C.; Sung, H. W. *J. Controlled Release* **2004**, *96*, 285.
32. Tang, Q.; Wu, J.; Sun, H.; Fan, S.; Hu, D.; Lin, J. *Carbohydr. Polym.* **2008**, *73*, 473.
33. Rodriguez, D. E.; Romero-Garcia, J.; Ramirez-Vargas, E.; Ledezma-Perez, A. S.; Arias-Marin, E. *Mater. Lett.* **2006**, *60*, 1390.
34. Neamtu, I.; Chiriac, A. P.; Nita, E. *J. Optoelectron. Adv. Mater.* **2006**, *8*, 1939.
35. Lin, Z.; Wu, W.; Wang, J.; Jin, X. *Frontiers Mater. Sci. China* **2007**, *1*, 427.

36. Suzuki, A.; Hara, T. *J. Chem. Phys.* **2001**, *114*, 5012.
37. Tazhbaev, E. M.; Mustafin, E. S.; Burkeev, M. Z.; Russ, B. K. *J. Phys. Chem.* **2006**, *80*, 1300.
38. Hu, D. S. G.; Lin, M. T. S. *Polymer* **1994**, *35*, 4416.
39. Lin, Z. H.; Wu, W. H.; Wang, J. Q.; Jin, X. *React. Funct. Polym.* **2007**, *67*, 789.
40. Siegel, R. A.; Firestone, B. A. *Macromolecules* **1988**, *21*, 3254.
41. Park, T. G.; Hoffman, A. S. *J. Appl. Polym. Sci.* **1992**, *46*, 659.
42. Suzuki, H.; Wang, B.; Yoshida, R.; Kokufuta, E. *Langmuir* **1999**, *15*, 4283.
43. Feil, H.; Bae, Y. H.; Feijen, J.; Kim, S. W. *Macromolecules* **1993**, *26*, 2496.
44. Taylor, L. D.; Cerankowski, L. D. *J. Polym. Sci. Part A: Polym. Chem.* **1975**, *16*, 2551.
45. Emileh, A.; Farahani, E. V.; Imani, M. *Eur. Polym. J.* **2007**, *43*, 1986.
46. Fessi, H.; Devissaguet, J. P.; Puisieux, F. U.S. Pat. 5,118,528 (**1992**).
47. Mahdavinia, G. R.; Zohuriaan-Mehr, M. J.; Pourjavadi, A. *Polym. Adv. Technol.* **2004**, *15*, 173.
48. Caykara, T.; Kiper, S.; Demirel, G. *Eur. Polym. J.* **2006**, *42*, 348.
49. Serra, L.; Doménech, J.; Peppas, N. A. *Biomaterials* **2006**, *27*, 5440.
50. Cai, W. S.; Gupta, R. B. *Ind. Eng. Chem. Res.* **2001**, *40*, 3406.
51. Lin, Z. H.; Wu, W. H.; Wang, J. Q.; Jin, X. *Fine Chem.* **2007**, *24*, 1043.